CrossMark

ORIGINAL ARTICLE

Nitrous oxide (N$_2$O) emissions from a mesotrophic reservoir on the Wujiang River, southwest China

Xiaolong Liu[1] · Siliang Li[2] · Zhongliang Wang[1] · Guilin Han[3] · Jun Li[1] ·
Baoli Wang[2] · Fushun Wang[4] · Li Bai[1]

Abstract Aquatic ecosystems have been identified as a globally significant source of nitrous oxide (N$_2$O) due to continuous active nitrogen involvement, but the processes and influencing factors that control N$_2$O production are still poorly understood, especially in reservoirs. For that, monthly N$_2$O variations were monitored in Dongfeng reservoir (DFR) with a mesotrophic condition. The dissolved N$_2$O concentration in DFR displayed a distinct spatial–temporal pattern but lower than that in the eutrophic reservoirs. During the whole sampling year, N$_2$O saturation ranging from 144% to 640%, indicating that reservoir acted as source of atmospheric N$_2$O. N$_2$O production is induced by the introduction of nitrogen (NO$_3^-$, NH$_4^+$) in mesotrophic reservoirs, and is also affected by oxygen level and water temperature. Nitrification was the predominate process for N$_2$O production in DFR due to well-oxygenated longitudinal water layers. Mean values of estimated N$_2$O flux from the air–water interface averaged 0.19 μmol m^{-2} h^{-1} with a range of 0.01–0.61 μmol m^{-2} h^{-1}. DFR exhibited less N$_2$O emission flux than that reported in a nearby eutrophic reservoir, but still acted as a moderate N$_2$O source compared with other reservoirs and lakes worldwide. Annual emissions from the water–air interface of DFR were estimated to be 0.32×10^5 mol N–N$_2$O, while N$_2$O degassing from releasing water behind the dam during power generation was nearly five times greater. Hence, N$_2$O degassing behind the dam should be taken into account for estimation of N$_2$O emissions from artificial reservoirs, an omission that historically has probably resulted in underestimates. IPCC methodology should consider more specifically N$_2$O emission estimation in aquatic ecosystems, especially in reservoirs, the default EF5 model will lead to an overestimation.

Keywords Nitrous oxide · Mesotrophic reservoir · Nitrogen dynamics · IPCC methodology

✉ Xiaolong Liu
liu_xiaolong@126.com

✉ Siliang Li
siliang.li@tju.edu.cn

1 Tianjin Key Laboratory of Water Resources and Environment, Tianjin Normal University, Tianjin 300387, China

2 Institute of Surface-Earth System Science, Tianjin University, Tianjin 300072, China
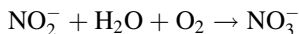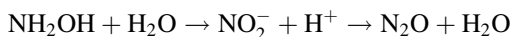
3 School of Scientific Research, China University of Geosciences (Beijing), Beijing 100083, China

4 Applied Radiation Institute, School of Environmental and Chemical Engineering, Shanghai University, Shanghai 200433, China

1 Introduction

River impoundment and dam construction have significantly altered the aquatic environment and water dynamics during recent decades, resulting in complex feedback mechanisms on nitrogen biogeochemical cycles. In 1996, there were approximately 42000 large dams in rivers worldwide (Rosenberg et al. 2000). Hydroelectric power was accepted as "green energy" for a long time, but in recent years researchers have noted associated deterioration of water quality and aquatic environments, including eutrophication and greenhouse gas (GHG) emissions (Liu et al. 2011a; Wang et al. 2011; Beaulieu et al. 2015; Fearnside 2016). Indeed, most of the hydroelectric reservoirs worldwide have been identified as potentially important sources GHGs, including CO$_2$, CH$_4$, and nitrous oxide (N$_2$O) (Peng et al. 2012; Sturm et al. 2014; Beaulieu

🖄 Springer

et al. 2015; Fearnside 2016; Musenze et al. 2016). Aquatic N_2O production and emissions at reservoirs have attracted additional attention recently as increased nitrogen loading in reservoirs has resulted from anthropogenic activity (Beaulieu et al. 2015).

N_2O, a powerful GHG that contributes significantly to the destruction of stratospheric ozone (Ravishankara et al. 2009), is an important component of nitrogen loss during aquatic nitrogen biogeochemical cycling. Although atmospheric N_2O concentration is lower than CO_2, its global warming potential is about 298 times greater than CO_2 (IPCC 2006). Atmospheric mixing ratios of N_2O have been increasing steadily over the past century. Aquatic systems contribute 25%–30% of total global N_2O emissions (IPCC 2006).

N_2O is mainly produced during microbial processes such as nitrification and denitrification. Nitrification is an aerobic process through which ammonium is oxidized to nitrate. During this process, N_2O is a by-product of the oxidation of NH_4^+ by nitrifying bacteria and methanotrophs (Mengis et al. 1997). The yield of N_2O in nitrification strongly depends on the concentrations of dissolved oxygen and nitrate. The processing steps of nitrification are:

$$NH_4^+ + O_2 \rightarrow NH_2OH + H^+$$

$$NH_2OH + H_2O \rightarrow NO_2^- + H^+ \rightarrow N_2O + H_2O$$

$$NO_2^- + H_2O + O_2 \rightarrow NO_3^-$$
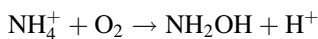
In suboxic conditions, nitrate can be reduced by denitrification to molecular nitrogen, with N_2O as an intermediate. The rate of denitrification is influenced by temperature, abundance of organic carbon, and supply of N. As an intermediate in denitrification (NO_3^- to N_2), N_2O may accumulate when O_2 is present along with high NO_3^- concentrations:

$$NO_3^- \rightarrow NO_2^- \rightarrow NO \rightarrow N_2O \rightarrow N_2$$
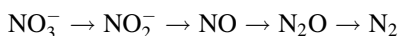
Nitrification and denitrification often occur simultaneously in aquatic ecosystems, especially in periodically thermally stratified deep reservoirs (depth >30 m) (Liu et al. 2011a; Beaulieu et al. 2015). Factors controlling N_2O yield, including temperature, available dissolved oxygen, nitrogen variation, and organic matter, vary temporally and spatially in reservoirs, and little is known about their specific impacts on N_2O yield in reservoirs. While N_2O is enhanced by increasing N levels and increasing eutrophication, this connection is not well characterized. Reservoirs are complex and dynamic ecosystems and it is important to understand how they operate and respond to changes in order to make appropriate management decisions.

Calculated N_2O emissions from China are globally significant, accounting for over 90% of those in the Pacific

Basin (Seitzinger and Kroeze 1998), but there is still considerable uncertainty or overestimation as few studies of N_2O production and emission have been made in China's reservoirs (Liu 2007; Liu et al. 2011a). The objectives of our study are: (1) to ascertain the spatial and temporal variations of N_2O emission and assess whether the reservoir functions as a sink or a source of N_2O, (2) to understand the impact of nitrogen dynamics on N_2O emissions, and (3) to assess the production mechanisms of N_2O and influential factors.

2 Study area and methods

2.1 Study area

The Wujiang is one of the largest tributaries in the upper reaches of the Changjiang Basin, mainly flowing through a karst area in Guizhou Province, with a total length of 874 km, drainage area of 66849 km^2, and mean water discharge of 1690 m^3 s^{-1}. The karst landscape accounts for about 70% of the total drainage area of the Wujiang River, and water chemistry is controlled by carbonate dissolution under the influence of carbonic and sulfuric acid (Han et al. 2010). The region experiences a subtropical monsoon humid climate, with perennial mean temperature of 14.8 °C and multi-year average annual rainfall of about 1100 mm. Dongfeng reservoir (DFR) (26°51′N, 106°8′E), located in Qingzhen City, Guizhou Province, was completed in 1994. It has a surface area of 19.06 km^2, a total volume of 8.63×10^8 m^3, and drainage area of 18161 km^2.

2.2 Sampling

Samples were collected monthly from July 2007 to June 2008 (Fig. 1) from the central part of the river, generally 0.4–0.5 km upstream of the dam at depths of 0.5, 5, 15, 30, and 60 m using a Niskin bottle. Samples downstream of the dam were collected 0.5 m under the water surface. In total, 60 vertical samples and 12 downstream samples were collected.

2.3 Environmental variables and nitrogen species

Water temperature (T), pH, dissolved oxygen (DO), and chlorophyll levels were measured in situ using an automated multi-parameter monitoring instrument (United States Gimcheon Instruments Inc. YSI 6600 v2). Water samples were filtered through 0.70-μm membrane filters (Whatman), H_2SO_4 was added (pH < 2), and the samples were cold-stored at <4 °C in the dark until analyzed. The concentrations of NO_3^- were measured using an automatic flow analyzer (SKALAR Sans Plus Systems), with
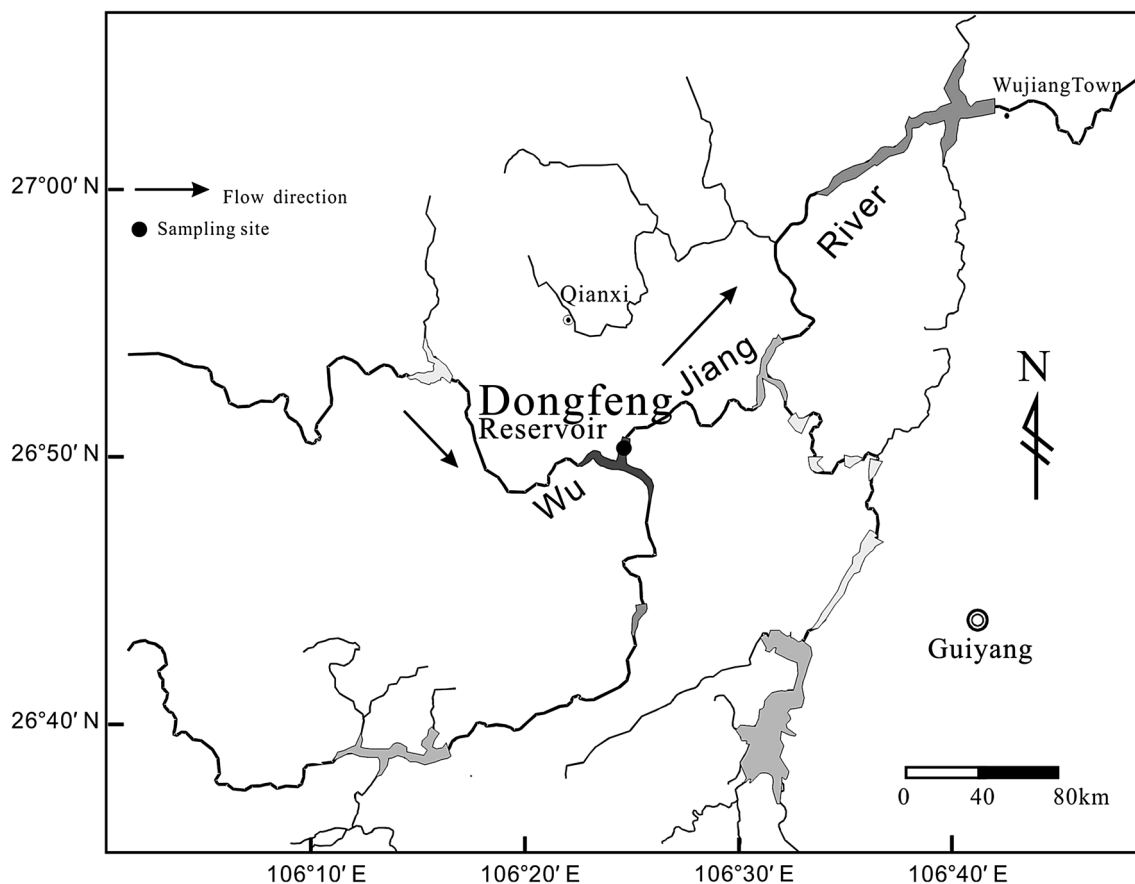
Fig. 1 Map showing the location of Dongfeng reservoir on the Wujiang River

precision under 2% as determined by duplicate samples. In addition, total phosphorous (TP) was determined spectrophotometrically (Unico UV-2000) using the molybdenum blue method after alkaline potassium persulfate digestion. Total nitrogen (TN) was also analyzed spectrophotometrically (Unico UV-2000) after alkaline potassium persulfate digestion. The typical precision of TN and TP measured by the spectrophotometric method is ±3%.

2.4 N$_2$O measurement and flux calculation

N$_2$O concentration in water was measured following the headspace-GC method. Water samples were collected in serum bottles, amended with 10 mol L^{-1} sodium hydroxide (NaOH) as a preservative, and sealed with rubber stoppers. The headspace equilibrium technique was used to determine the concentrations of dissolved gases. Details are available in Liu et al. (2011a) and Wang et al. (2009). The relative errors for N$_2$O measurement were less than 2%; regression corrections with ambient air were less than ± 10 nmol L^{-1}.

For assessing N$_2$O concentration and saturation, gas concentrations were expressed as the degree of saturation relative to air (Mengis et al. 1997):

$$\text{Degree of N}_2\text{O}_{\text{saturation}} = C_{N_2O}/C_{N_2Oatm} \times 100 \quad (1)$$

$$C_{N_2Oatm} = K \times C_A \quad (2)$$

where C_{N2O} is the measured concentration, C_{N2Oatm} is the saturated concentration of N$_2$O in water at the given water temperature and C_A is the atmospheric N$_2$O concentration of the sampling sites. The saturated concentration of N$_2$O in water was calculated using Henry's Law, where K is the Bunsen coefficient.

Apparent oxygen utilization (AOU) and ΔN$_2$O were calculated as follows:

$$AOU = DO_{sat} - DO_{meas} \quad (3)$$

$$\Delta N_2O = C_{N_2O} - C_{N_2Oatm} \quad (4)$$

where DO_{sat} is the saturation DO concentration in water and DO_{meas} is the measured concentration of DO.

The exchange flux of N$_2$O at the gas–water boundary layer of the surface water was calculated as:

$$F = K\Delta C = \frac{D}{Z}(C_s - C_{eq}) \tag{5}$$

$$D = 5.06 \times 10^{-9}\frac{T}{\eta V_b^{0.6}} \tag{6}$$

where F is the gas exchange flux; ΔC is the difference between the N_2O concentration in the air and water; K is the gas transfer velocity; D is the gas diffusion coefficient, which was calculated using Eq. (6), obtained from Lerman (1979); η is the viscosity of the water; V_b is the molar volume of the gas, with a value of 36.4 cm^3 mol^{-1} (Satterfield 1970); and Z is the thickness of the boundary layer, which is an empirical constant related to wind speed (Emerson 1975). Taking into account variations in wind speed for each sampling month, Z was estimated to have a value of 180–350 μm.

2.5 Statistical analysis

Statistical analysis was conducted using SPSS Statistics 22.0.0, Grapher 12.0, and Microsoft Excel in Windows 10. In all analyses where $p < 0.05$, the factor and the relationship tested were considered statistically significant.

3 Results

3.1 Variation of water parameters and trophic status

Surface water parameters including temperature, pH, chlorophyll, and DO displayed significant monthly variation (Fig. 2). Monthly variation data were divided into two groups: cold season (November to March) and warm season (April to October). DO, pH, and chlorophyll in the cold season ranged from 188.75 to 323.75 μmol L^{-1} (average 281.65 μmol L^{-1}), 7.50–8.73 (average 7.83), and 0.01–2.20 μg L^{-1} (average 0.24 μg L^{-1}), respectively. In warm season, DO, pH, and chlorophyll ranged from 209.69 to 337.50 μmol L^{-1} (average 271.38 μmol L^{-1}), 7.25–8.73 (average 7.88), and 0.05–6.60 μg L^{-1} (0.93 μg L^{-1}), respectively. All three parameters were generally higher in the warm season than in the cold season. Temperature, pH, DO, and chlorophyll in DFR surface waters shared similar seasonal trends with the Hongjiadu (HJD) and Wujiangdu (WJD) reservoirs on the mainstem of the Wujiang River (Liu et al. 2011a) and with reservoirs in the Maotiao River (Wang et al. 2011, 2015). However, DFR had higher DO and lower pH than HJD; and lower DO, pH, and chlorophyll than WJD.

DFR was typically thermally stratified in spring (April to June) and summer (July to September) during the sampling year. Thermal stratification was absent from October to March (Fig. 4). pH and DO showed similar vertical

distribution. In thermally stratified months, pH and DO values were lower in the deep water layers than in surface waters, e.g. mean values of 7.69 and 242.14 μmol L^{-1}, respectively, in the bottom layer, and of 8.38 and 296.15 μmol L^{-1} in surface waters. Compared with HJD and WJD, pH and DO in the bottom layer of DFR were much higher (Liu et al. 2011a), perhaps because DFR is much deeper (>100 m) than the others. DO data suggest that deep waters (depth of 60 m) maintained anoxic environment.

Results for TN, TP, and chlorophyll concentrations are in Fig. 3. TN and TP in DFR surface waters ranged from 2.30 to 5.11 mg L^{-1} (average 3.50 mg L^{-1}) and 0.001–0.31 mg L^{-1} (average 0.04 mg L^{-1}), respectively. Significant monthly variation in TP and chlorophyll were observed, suggesting eutrophic status varied greatly between cold seasons and warm seasons. DFR had moderate TN, TP, and chlorophyll content when compared with HJD and WJD (Liu et al. 2011a). However, as discussed and reported previously, reservoirs along Wujiang River have higher nitrogen loading than other reservoirs, such as Harsha Lake (Beaulieu et al. 2014), and Three Gorges reservoir (Zhu et al. 2013). Comparable high nitrogen loading has been reported in other watersheds and reservoirs, such as Brookville Lake and Mississinewa (Beaulieu et al. 2015). The main nitrate sources in the Wujiang watershed are nitrification and flooded soil organic matter (Li et al. 2010). The moderate levels of TN, TP, and chlorophyll in DFR indicate that the reservoir has a mesotrophic nutrient status when compared to its upstream (HJD) and downstream (WJD) counterparts. Chlorophyll was only detected in the upper layer (>15 m); average concentrations in thermal stratification months and non-thermal stratification months were 2.23 and 0.46 μg L^{-1}, respectively. In comparison, chlorophyll in WJD and HJD in the warm season averaged 20.45 and 2.66 μg L^{-1}, respectively, and in the cold season, 1.01 and 0.53 μg L^{-1}. The concentration of chlorophyll in DFR is very similar to HJD, an oligotrophic reservoir, but is notably lower than WJD, a eutrophic reservoir.

3.2 Monthly and spatial variation of N_2O in the reservoir

Significant vertical and monthly variation of N_2O concentration was observed in DFR (Fig. 3). All surface waters were supersaturated with respect to the equilibrium atmospheric N_2O concentration, 319 ppbv (IPCC 2006). The N_2O concentration in surface waters ranged from 15.05 to 59.63 nmol L^{-1} (average 27.03 nmol L^{-1}); corresponding N_2O saturations were from 164.79% to 640.89% (average 287.31%), indicating that DFR represents a N_2O source to the atmosphere.

Fig. 2 Monthly variations of environmental variables in surface waters
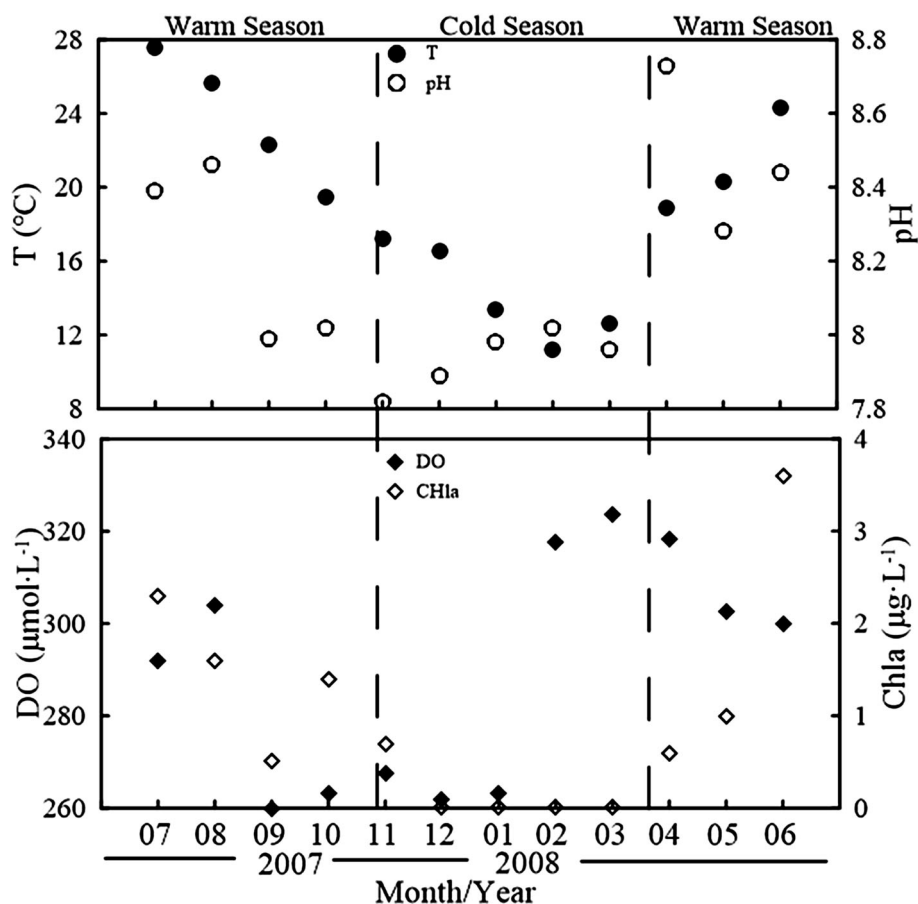
Significant vertical variation of N_2O was observed throughout the sampling year. Monthly average N_2O concentration in the deep water (depth >30 m) was significantly higher than that in surface waters (t test, $p < 0.05$), except in April and February. These anomalies were possibly due to N_2O accumulation in the hypolimnion where gas diffusion was constrained by the water density gradient. There was no apparent seasonal variation pattern of N_2O throughout the sampling year (Fig. 4). In the cold season, average surface-water N_2O concentration was 26.02 nmol L^{-1}, while in the warm season it was 28.03 nmol L^{-1}. Longitudinal averaged N_2O concentration in the cold season was 28.40 nmol L^{-1}, in contrast with 30.11 nmol L^{-1} in the warm season.

In general, N_2O concentration and saturation in DFR were conspicuously lower than in the WJD reservoir and slightly higher than in the HJD reservoir (Liu et al. 2011a). As previously noted, DFR is classified as a mesotrophic reservoir while HJD is oligotrophic and WJD eutrophic, suggesting that N_2O concentration may differ according to nutrient status, with eutrophic having the highest N_2O saturation potential. This is coincident with the findings in Swiss lakes and reservoirs by Mengis et al. (1997), who concluded that oligo-

mesotrophic reservoirs had significantly lower N_2O saturation than eutrophic ones. In addition, DFR had slightly higher N_2O concentration and saturation than Ohio River basin oligotrophic reservoirs ($4 < NO_{2,3} < 19$ µg N L^{-1}; N_2O saturation ratio 0.4–2.0), but significantly lower than Ohio River basin mesotrophic and eutrophic reservoirs ($16 < NO_{2,3} < 1786$ µg N L^{-1}; N_2O saturation ratio 0–1000) (Beaulieu et al. 2014).

3.3 N_2O diffusion fluxes

Conservative estimates of N_2O flux in DFR were based on wind speed data provided by the meteorological observatory and on surface water N_2O saturation (Fig. 5). Monthly N_2O flux on the water–air interface ranged from 0.01 to 0.61 µmol m^{-2} h^{-1}, with an average value of 0.19 µmol m^{-2} h^{-1}. The highest emission flux was in April, while the lowest was in October, both turnover months between thermal and non-thermal stratified periods. No obvious seasonal difference in N_2O flux was exhibited. Compared to the average surface flux in surface waters of adjacent reservoirs WJD and HJD (0.67 µmol m^{-2} h^{-1} and 0.45 µmol m^{-2} h^{-1}, respectively), DFR had notably lowest emission level of the three reservoirs.

Fig. 3 Monthly variation of TN, TP, and Chlorophyll in Dongfeng reservoir
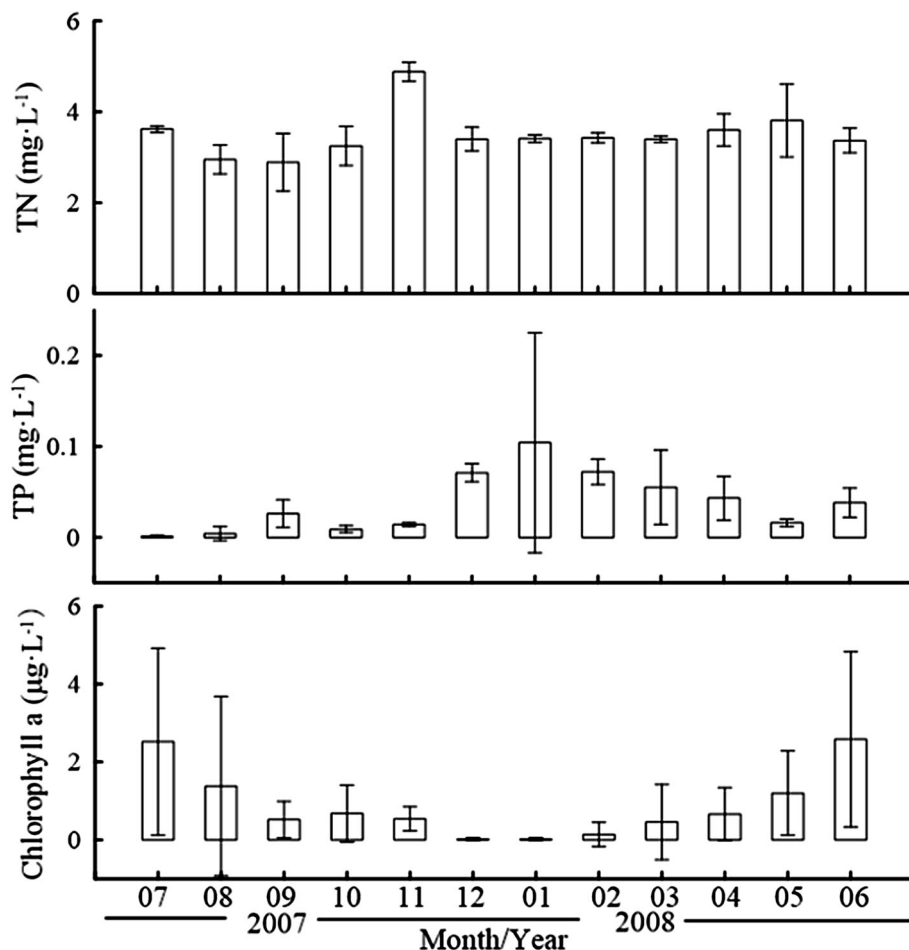
4 Discussion

4.1 Effects of nitrogen and environment variables on N₂O

Environmental variables such as T, DO, and nitrogen species are known to influence N_2O production and emissions in artificial reservoirs (Liu et al. 2011a ; Zhu et al. 2013; Beaulieu et al. 2014, 2015). The relationships between N_2O concentration and nitrogen species, T, and DO in DFR were analyzed (Fig. 6); T and DO were recognized as the two most important factors for spatial and temporal N_2O variation. T was found to have a significant negative correlation with N_2O concentration in summer and spring (R = 0.55; P = 0.003), while a positive correlation in winter (R = 0.70; P = 0.004). DO in DFR also had a negative correlation with N_2O in summer and autumn (R = 0.63; P < 0.001), while a positive correlation in spring (R = 0.60; P = 0.002). Seasonal differences in the relationships of T and DO with N_2O may be related to the complexity of N_2O production throughout the water column. T exhibited an opposite correlation with N_2O in warm seasons versus winter probably due to significant differences of N_2O between surface waters and deep waters in warm seasons while this phenomena disappeared in winter (Fig. 4). Good correlation between T and N_2O in surface waters was also found in Three Gorges reservoir (Zhu et al. 2013), but this correlation has not held in other reservoirs worldwide (Huttunen et al. 2002; Hendzel et al. 2005; Guerin et al. 2008; Liu et al. 2011a; Zhu et al. 2013; Beaulieu et al. 2014). Actually, N_2O production mainly occurs in the water column in reservoirs, especially in the hypolimnion (Deemer et al. 2011; Beaulieu et al. 2014), thus the influence of temperature and DO on N_2O production also depends on other parameters such as nitrogen loading in water layers and dissolved organic carbon content.

The relationships of N_2O with NO_3^- and NH_4^+ in different seasons were analyzed at DFR (Fig. 6). We found a good and positive relationship between N_2O and NO_3^- in autumn (R = 0.63; P = 0.016), with the exception of one deep-water sample at 60 m (Fig. 6). Positive correlations between N_2O and NO_3^- are well documented in rivers and streams (Yu et al. 2013; Liu et al. 2015), lakes (Wang et al. 2009), and reservoirs (Liu et al. 2011a; Beaulieu et al. 2015). Nitrification and denitrification have been identified as the major N_2O-producing pathways in reservoirs (Mengis et al. 1997; Deemer et al. 2011; Liu et al. 2011a;
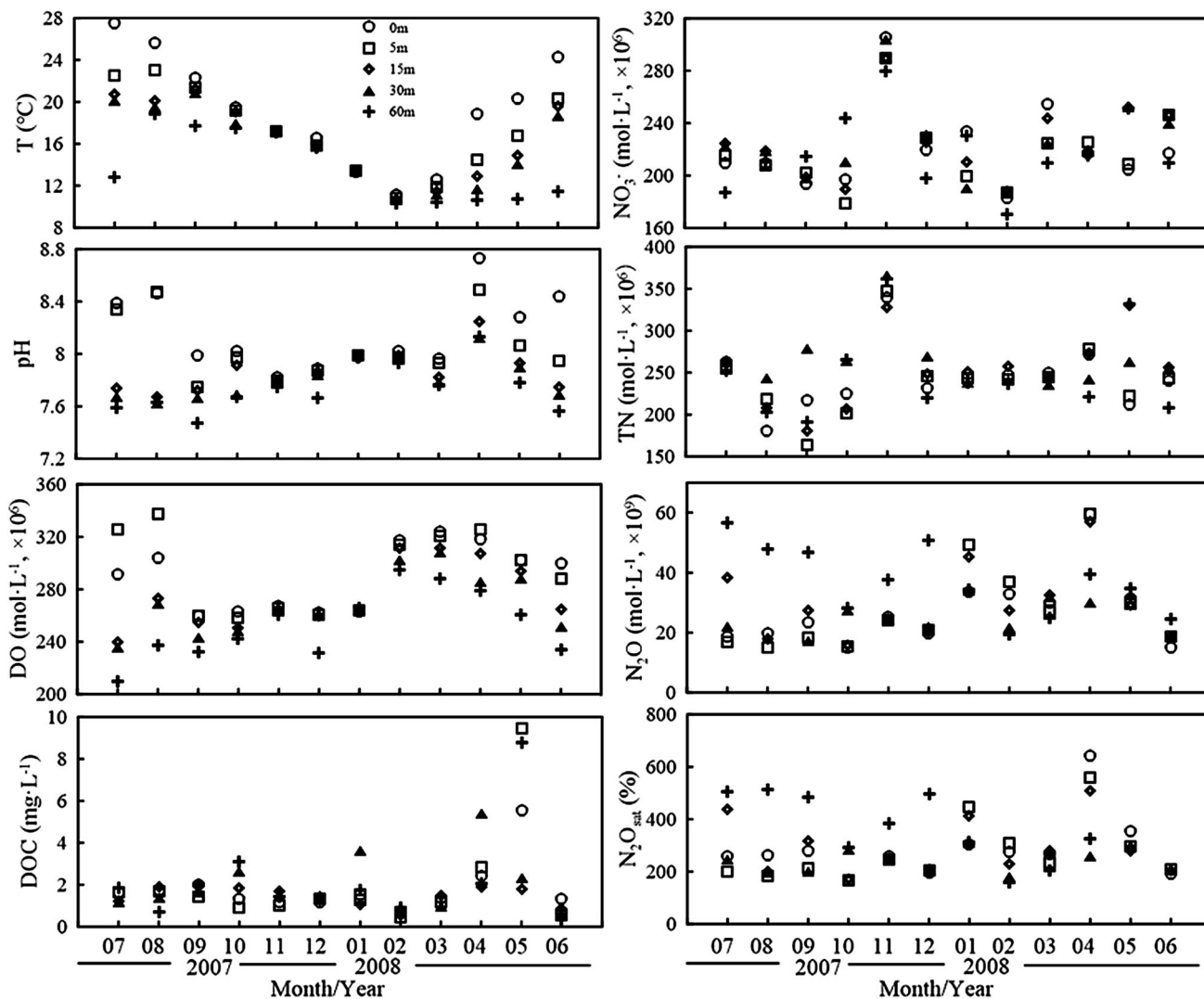
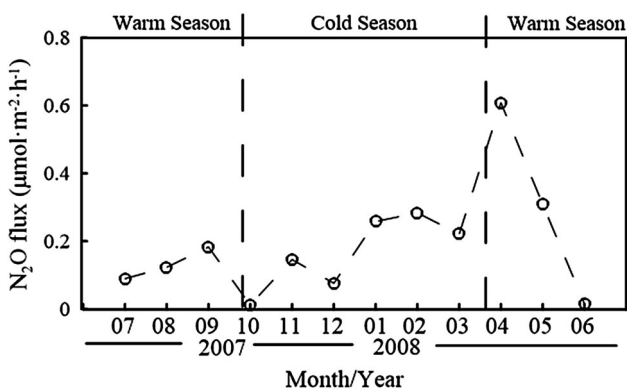Fig. 4 Longitudinal and monthly distribution pattern of N₂O and main parameters

Fig. 5 N₂O concentration, saturation, and emission flux in surface waters

Beaulieu et al. 2014), and NO_3^- should have a positive correlation with N₂O, especially in nitrification-dominated aquatic environments. However, in DFR, a significant relationship was observed between N₂O and NO_3^- only in autumn, which was likely due to N₂O being produced by both nitrification and denitrification, resulting in disproportionate NO_3^- consumption and production with N₂O production. Excess NO_3^- and exogenous nitrogen input into a reservoir also result in this disproportionation.

A positive correlation between N₂O and NH_4^+ ($R = 0.82$; $P < 0.001$) was identified in the warm season (from April to September) with a slope of 1.13 (Fig. 6). As previously noted, the water column remained oxic throughout the year, even during the thermal stratification period. A well-oxygenated water column provides ideal conditions for NH_4^+ oxidation. The first step of nitrification is the oxidation of NH_4^+ to hydroxylamine (NH_2OH), during which both NO_2^- and N₂O are produced. If the NO_2^- is not immediately oxidized to NO_3^-, reduced to N₂O or N₂ (nitrifier-denitrification), or assimilated into biomass, NH_4^+ oxidation results in the simultaneous
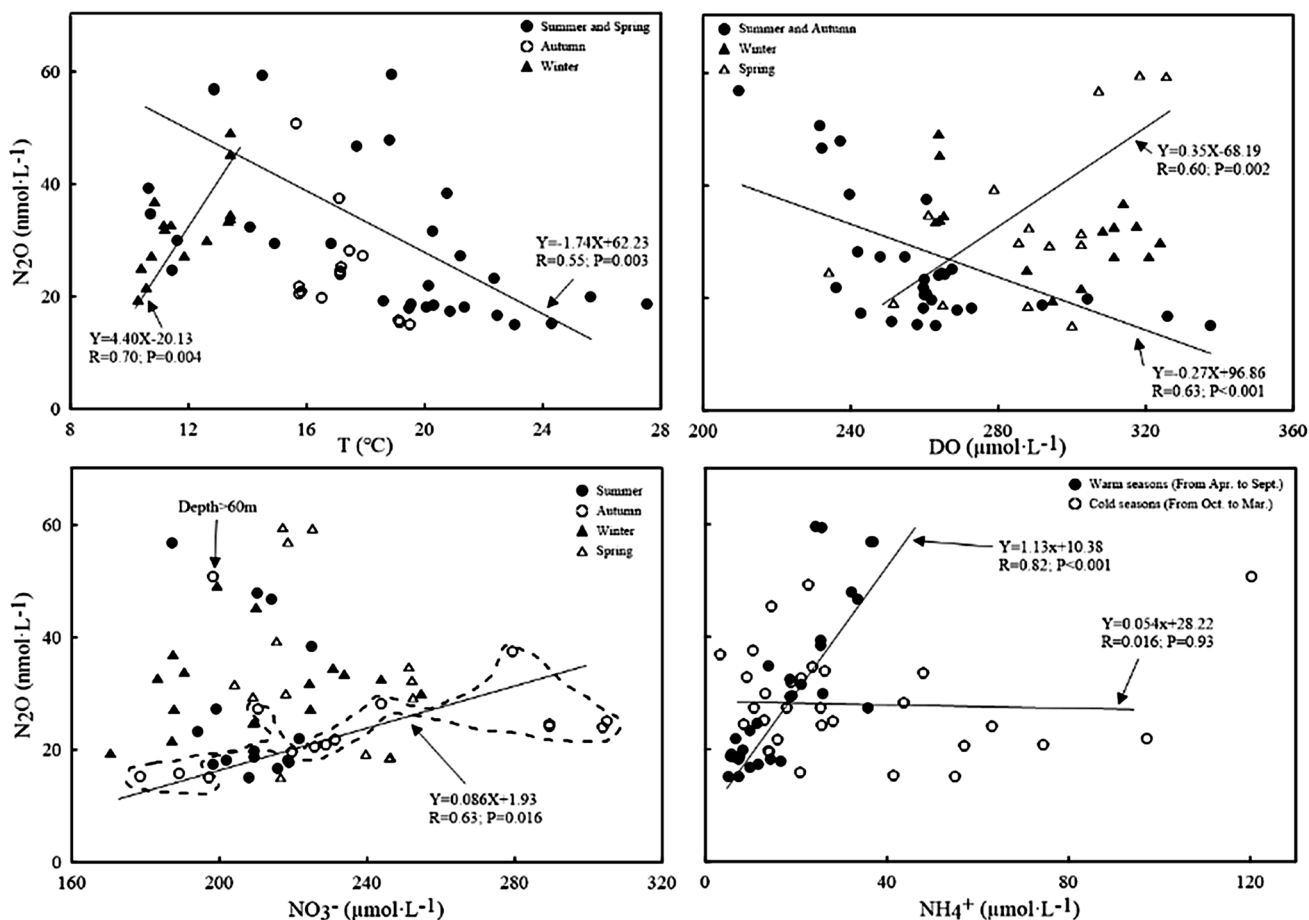
Fig. 6 Correlation of N$_2$O with nitrogen and T, DO in Dongfeng reservoir

accumulation of N$_2$O and NO$_2^-$ (Sasaki et al. 2011; Beaulieu et al. 2015). In other words, NH$_4^+$ promotes N$_2$O production in oxygenated water layers when sufficient NH$_4^+$ is available. But in cold seasons, the mineralization process, which produces NH$_4^+$ through organic matter decomposition in anaerobic water layers, would be blocked by well-oxygenated waters and water-mixing processes.

4.2 Production mechanisms of N$_2$O

As previously noted, denitrification is not a dominant process for N$_2$O production, but how it might influence spatial and temporal N$_2$O distribution in DFR still unknown. That is to say, whether nitrification is solely responsible for N$_2$O in this mesotrophic reservoir remains to be determined. A linear correlation between ΔN$_2$O and AOU in oxic waters has established that N$_2$O is produced by nitrification in oceans, lakes, rivers, and reservoirs. AOU reflects the amount of O$_2$ consumed by remineralization of organic matter and nitrification, while the strong correlation between AOU and ΔN$_2$O commonly observed in depth profiles provides circumstantial evidence that

nitrification is the dominant mechanism of N$_2$O production in oceans (Nevison et al. 2003), lakes (Mengis et al. 1996; Wang et al. 2009), and reservoirs (Mengis et al. 1997; Liu et al. 2011). The reported regression coefficient varies from 0.076 to 0.31 nmol L^{-1} ΔN$_2$O/μmol L^{-1} AOU (Suntharalingam and Sarmiento 2000).

In Fig. 7, ΔN$_2$O was plotted versus AOU for all water samples throughout the reservoir. While a considerable amount of scatter appears on the figure, significant positive correlation between AOU and ΔN$_2$O was found in the sampling year with the exception of spring. A good linear correlation was found in summer (R = 0.75; P = 0.001; July to September) in DFR; the calculated regression coefficient was 0.19 nmol L^{-1} ΔN$_2$O/μmol L^{-1} AOU. A significant positive correlation between AOU and ΔN$_2$O was also found in the cold season (R = 0.41; P = 0.023; October to March), with a calculated regression coefficient of 0.23 nmol L^{-1} ΔN$_2$O/μmol L^{-1} AOU. The regression coefficients for reservoirs in this study agree nicely with reported coefficients in lakes and oceans (Mengis et al. 1997; Nevison et al. 2003; Wang et al. 2009; Liu et al. 2011), indicating that N$_2$O production in DFR was
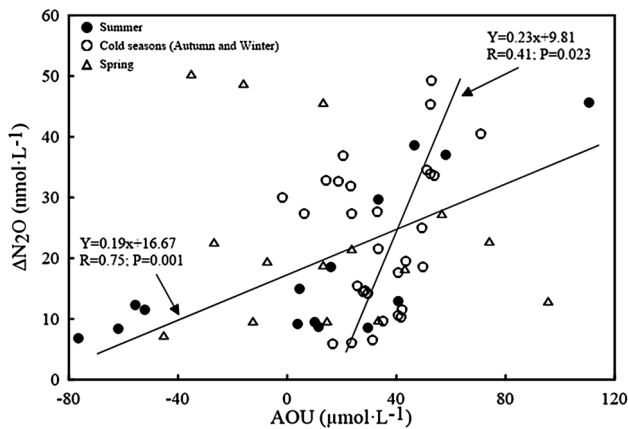
Fig. 7 ΔN_2O versus AOU in Dongfeng reservoir

predominated by nitrification. In addition, even though N_2O only correlated with NO_3^- in autumn, it exhibited a wide-ranging positive correlation with NH_4^+, which supports N_2O production by nitrification.

This approach for identifying the key process of N_2O production is not definitive as numerous factors can contribute to the variability (Mengis et al. 1997). Organic matter that oxidized in different layers, or differences in the production yield of nitrifiers could result in varying $\Delta N_2O/$AOU ratios. In addition, mixing of different water masses or additional N_2O sources, such as denitrification or assimilative NO_3^- reduction, may also affect $\Delta N_2O/$AOU ratios.

4.3 N_2O–N:NO_3–N ratio for assessing N_2O production and IPCC methodology

The IPCC method for indirect N_2O emissions assumes that a certain proportion of soil nitrogen including anthropogenic fertilizer and organic nitrogen is leached to aquatic ecosystems, from which N_2O is produced and emitted from groundwater and surface drainages to rivers and estuaries (IPCC 2006). Indirect N_2O emissions from agricultural N utilization are estimated for groundwater, rivers, and estuaries using an emission factor (EF5) for aquatic ecosystems. Currently, EF5 is set at 0.75% (kg N_2O-N per kg N leached), with an uncertainty range of 0.05%–2.5% (IPCC 2006). Specifically, for each aquatic component, the aquatic EF5 values are currently 0.25% for groundwater and surface drainage (EF5-g), rivers (EF5-r), and estuaries (EF5-e) (IPCC 2006; Baulch et al. 2012). Recently, the IPCC method for estimating indirect N_2O emissions from aquatic systems came into dispute (Baulch et al. 2012; Hinshaw and Dahlgren 2013; Yu et al. 2013). The current EF5-r value was confirmed based on data primarily from

small river systems, but there remains great uncertainty in scaling these values to larger rivers (Hinshaw and Dahlgren 2013). Studies in Ohio rivers showed a three-fold overestimation of N_2O (Beaulieu et al. 2011), and in spring-fed rivers in New Zealand, only 0.01% of N_2O estimated by IPCC methodology was observed (Clough et al. 2007). This uncertainty could be even greater for impounded rivers with multiple reservoirs.

Ratios of dissolved N_2O–N:NO_3–N from groundwater and agricultural drainage water has been used to confirm the EF5 value; in many studies this ratio has been used directly to evaluate emissions in rivers and lakes (McCrackin and Elser 2011), but few studies have focused on reservoirs. The N_2O–N:NO_3–N ratio in DFR over the study year ranged from 1.4×10^{-4} to 6.1×10^{-4}, with an average value of 2.7×10^{-4}, much lower than the default EF5 value of 75×10^{-4}, and even above the minimum value of 5×10^{-4}, suggesting an overestimation by IPCC methodology for reservoirs. Table 1 compares N_2O-N: NO_3-N ratios presented in recent literature. N_2O-N: NO_3-N ratios in HJD, WJD, and DFR along the Wujiang River exhibited lower values than default ratio values from IPCC methodology, suggesting that N_2O fluxes from reservoirs in Wujiang River would be significantly overestimated by the IPCC method. Similar overestimate would also happen in Swiss reservoirs (Mengis et al. 1997) and in Taihu Lake in China (Wang et al. 2009), where N_2O-N: NO_3-N ratios averaged 0.002 (Fig. 1). However, for reservoirs in the United States and Finland, default IPCC values would lead to an underestimate (Huttunen et al. 2002; Deemer et al. 2011).

The N_2O-N: NO_3-N ratios vary substantially among different reservoirs worldwide, contributing to poor understanding of N_2O emissions and spatiotemporal patterns, e.g. how the ratio of N_2O-N: NO_3-N varies seasonally and vertically within a reservoir is still unknown and the key influencing factors still not well understood. Significant negative correlation was observed between N_2O–N:NO_3–N ratios and T throughout the year in DFR (R = 0.45; P = 0.013 in cold season; R = 0.50; P = 0.005 in warm season) (Fig. 8). T seemed to constrain N_2O formation by NO_3 in the reservoir. However, DO displayed a much more complicated seasonal variation. Negative correlation was observed in summer (R = 0.71; P = 0.004) and winter and autumn (R = 0.81; P < 0.001) (Fig. 8). Nitrification was recognized as the dominant process for N_2O production in DFR and a positive correlation between N_2O–N:NO_3–N ratios and DO was observed in spring, indicating that DO increases N_2O–N:NO_3–N ratios. Further research is needed to confirm this relationship.

Table 1 Comparison of the ratio of N$_2$O-N: NO$_3$-N among different studies

Name of lake/reservoir	Location	Ratio of [N$_2$O–N]:[NO$_3$–N]		References
		Average	Range	
Dongfeng reservoir	China	0.00027	0.0001–0.0006	This study
Wujiangdu reservoir	China	0.00040	0.00017–0.0014	Liu et al. (2011a)
Hongjiadu reservoir	China	0.00045	0.00014–0.0031	Liu et al. (2011a)
26 lakes in Colorado	USA	0.01	0.001–0.07	McCrackin and Elser (2011)
Lacamas reservoir	USA	0.009	0.002–0.02	Deemer et al. (2011)
Taihu Lake	China	0.002	0.0003–0.02	Wang et al. (2009)
Lokaa reservoir	Finland	0.026	0.004–0.031	Huttunen et al. (2002)
Greifensee	Switzerland	0.002	0–0.017	Mengis et al. (1997)
IPCC indirect N$_2$O emission factor (EF5)	N/A	0.0025	0.0005–0.025	IPCC (2006)
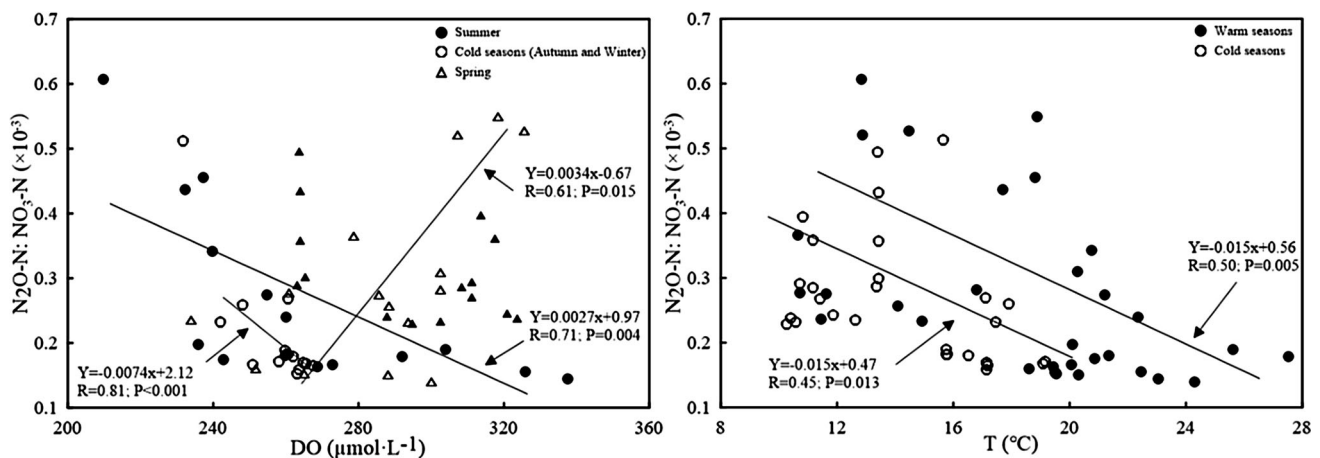
Fig. 8 Relationship between N$_2$O-N: NO$_3$-N ratios and T, DO

4.4 N$_2$O emission fluxes compared with other water bodies

Exchange fluxes of N$_2$O were estimated in DFR by month, as previously noted; maximum and minimum emission fluxes values were in April 2008 and October 2007, respectively. In April (early stage of thermal stratification), N$_2$O emission was expected to exhibit a supersaturation status and high emission flux, as found in other reservoirs (Liu et al. 2011a; Beaulieu et al. 2014), but this temporal pattern was complicated by variable nitrogen dynamics, especially in thermal stratification seasons. N$_2$O fluxes of other reservoirs and lakes worldwide are listed in Table 2. Tropical reservoirs tend to emit more N$_2$O through the water–air interface than subtropical and temperate reservoirs. In addition, DFR had rather low N$_2$O emission flux when compared to other subtropical reservoirs, including the adjacent WJD and HJD reservoirs. As many lakes and reservoirs worldwide, those in the Wujiang basin are subject to substantial N loading from the surrounding

watershed as evidenced by the high N levels in HJD, WJD, and DFR. Even though DFR is a mesotrophic reservoir, the N$_2$O production and saturation in the hyperlimnion maintained a high level when compared with the eutrophic WJD reservoir. However, the difference in N$_2$O emission fluxes between WJD and DFR indicates that nutrient status impacts N$_2$O production.

According to the N$_2$O emission fluxes and water surface area of DFR (19.06 km^2), we estimated the annual N$_2$O emissions from the water–air interface to be 0.32×10^5 mol N$_2$O. Due to a smaller water surface area and flux, annual N$_2$O emissions were less in DFR than in HJD and WJD (3.17×10^5 mol N$_2$O and 2.81×10^5 mol N$_2$O, respectively) (Liu et al. 2011a). Although this annual N$_2$O emission amount was not comparable with large rivers and soil systems, it should be emphasized since most rivers worldwide are impounded with reservoirs, especially in China. China is already the world's largest producer of hydroelectricity, with more than 220 large- and medium-scale (>50 MW) hydropower plants and over 40,000

Table 2 Emission fluxes of N_2O at water–air interface in lakes and reservoirs

Name	Location	Climate	FN$_2$O (μmol m^{-2} h^{-1})	References
Reservoirs				
Petit Saut	French Guiana	Tropical	4.04 ± 2.54	Guerin et al. (2008)
Fortuna	Panama	Tropical	0.29 ± 0.46	Guerin et al. (2008)
Tucurui	Brazil	Tropical	5.21 ± 3.42	Lima et al. (2002)
Samuel	Brazil	Tropical	6.54 ± 6.17	Lima et al. (2002)
Serra de Mesa	Brazil	Tropical	0.13 ± 0.92	Sikar et al. (2005)
Manso	Brazil	Tropical	0.13 ± 1.25	Sikar et al. (2005)
William H. Harsha	United States	Extratropical	$\approx -50 \sim \approx 100$ (data from fig)	Beaulieu et al. (2014)
Lokka	Finland	Temperate	$-0.08 \sim 0.26$	Huttunen et al. (2002)
Porttipahta	Finland	Temperate	$-0.02 \sim 0.24$	Huttunen et al. (2002)
Three Gorges	China	Subtropical	0.32 ± 0.48	Zhu et al. (2013)
Hongjiadu	China	Subtropical	$0.45 (0.10 \sim 1.32)$	Liu et al. (2011a)
Wujiangdu	China	Subtropical	$0.64 (0.08 \sim 1.76)$	Liu et al. (2011a)
Dongfeng	China	Subtropical	$0.19 (0.01 \sim 0.61)$	This study
Natural lakes				
Mochou	Antarctica	Frigid	0.22 ± 0.48	Liu et al. (2011b)
Tuanjie	Antarctica	Frigid	0.18 ± 0.20	Liu et al. (2011b)
Daming	Antarctica	Frigid	0.51 ± 0.49	Liu et al. (2011b)
ELA in Ontario	Canada	Temperate	<0.0033	Hendzel et al. (2005)
Kevaton	Finland	Temperate	$0.09 \sim 0.50$	Huttunen et al. (2003)
Tahu	China	Subtropical	$0.41–0.58$	Wang et al. (2009)
Yuqiao	China	Subtropical	$0.18 (-0.14$ to $0.89)$	Liu et al. (2015)

smaller-scale ones. Given the rate of dam construction, GHG emissions from hydroelectric reservoirs may have significant global impact (Hu and Cheng 2013).

In addition, supersaturated N_2O content in the bottom waters will be released into the atmosphere as water passing through the turbines and spillways is drawn from the lower layer, and downstream GHG emissions will occur as water is released under pressure below the dam (Liu et al. 2011a; Fearnside and Pueyo 2012). In 2007, the water output of DFR was about 5.02×10^9 m^3, and the average concentration of N_2O in discharged water was 31.04 nmol L^{-1}. In total, 1.56×10^5 mol N_2O was released through power generation, which is nearly five times the N_2O emissions from the water–air interface. A similar difference between N_2O degassing from water–air interface and releasing water during power generation was found in WJD and HJD, but DFR has the highest proportion of the three. This is mainly because DFR has larger output than the other two reservoirs, demonstrating that management of reservoir operations strongly affects N_2O degassing.

The annual electric energy production of DFR is 24.2×10^8 kW/h (http://192.168.4.1/gsgk/zjdz/3213.htm). Combined N_2O emissions from the water–air interface and degassing from releasing water during power generation was

1.88×10^5 mol N_2O. So, per 1 kW/h electrical power, DFR released 77.69 μmol N_2O, which was lower than both WJD and HJD (107.78 and 134.88 μmol/kW/h, respectively).

5 Conclusions

This study investigated the temporal and spatial variation of N_2O as well as controlling factors in a mesotrophic reservoir. Though as a mesotrophic reservoir, DFR acted as obvious N_2O sources with respect to atmosphere. However, N_2O emission fluxes in DFR were significantly lower than that in the neighboring eutrophic WJD reservoir, implying that eutrophication may enhance the N_2O emission. N_2O production in DFR was dominated by nitrification in well-oxygenated water layers, while no obvious effects of denitrification on N_2O emission were observed in DFR, which should be emphasized in future researches, especially in sediment–water interface.

IPCC methodology would seemingly lead to overestimation if it were applied in reservoirs of the Wujiang River, but this needs to be substantiated by further observation because it remains unclear 1) how seasonal and diurnal N_2O variation influence N_2O-N: NO_3-N ratios and

2) how some special events, such as ice-cover water, may affect N_2O production with respect to NO_3^-.

N_2O emission flux from the water–air interface and N_2O degassing from releasing water behind the dam during power generation should be given equal attention and emphasis. N_2O emission flux from surface waters is related to N_2O saturation and physical–chemical quality, while N_2O degassing during power generation is related to water output and N_2O saturation in releasing water layers.

Compliance with ethical standards

Conflict of interest The authors declare that they have no conflicts of interest to this work. We declare that we do not have any commercial or associative interest that represents a conflict of interest in connection with the work submitted.

References

Baulch HM, Schiff Sherry L, Maranger R, Dillon Peter J (2012) Testing models of aquatic N_2O flux for inland waters. Can J Fish Aquat Sci 69:145–160

Beaulieu JJ, Tank JL, Hamilton SK, Wollheim WM, Hall RO, Mulholland PJ, Peterson BJ, Ashkenas LR, Cooper LW, Dahm CN, Dodds WK, Grimm NB, Johnson SL, McDowell WH, Poole GC, Valett HM, Arango CP, Bernot MJ, Burgin AJ, Crenshaw CL, Helton AM, Johnson LT, O'Brien JM, Potter JD, Sheibley RW, Sobota DJ, Thomas SM (2011) Nitrous oxide emission from denitrification in stream and river networks. Proc Natl Acad Sci USA 108:214–219

Beaulieu JJ, Smolenski RL, Nietch CT, Townsend-Small A, Elovitz MS, Schubauer-Berigan JP (2014) Denitrification alternates between a source and sink of nitrous oxide in the hypolimnion of a thermally stratified reservoir. Limnol Oceanogr 59:495–506

Beaulieu JJ, Nietch CT, Young JL (2015) Controls on nitrous oxide production and consumption in reservoirs of the Ohio River Basin. J Geophys Res Biogeosci 120:1995–2010

Clough TJ, Buckthought LE, Kelliher FM, Sherlock RR (2007) Diurnal fluctuations of dissolved nitrous oxide (N_2O) concentrations and estimates of N_2O emissions from a spring-fed river: implications for IPCC methodology. Glob Change Biol 13:1016–1027

Deemer BR, Harrison JA, Whitling EW (2011) Microbial dinitrogen and nitrous oxide production in a small eutrophic reservoir: an in situ approach to quantifying hypolimnetic process rates. Limnol Oceanogr 56:1189–1199

Emerson S (1975) Chemically enhanced CO_2 gas exchange in a eutrophic lake: a general model. Limnol Oceanogr 20:743–753

Fearnside PM (2016) Greenhouse gas emissions from Brazil's Amazonian hydroelectric dams. Environ Res Lett 11: 011002. doi:10.1088/1748-9326/11/1/011002

Fearnside PM, Pueyo S (2012) Greenhouse-gas emissions from tropical dams. Nature Clim Change 2:382–384

Guerin F, Abril G, Tremblay A, Delmas R (2008) Nitrous oxide emissions from tropical hydroelectric reservoirs. Geophys Res Lett 35:L06404. doi:10.1029/2007GL033057

Han G, Tang Y, Xu Z (2010) Fluvial geochemistry of rivers draining karst terrain in Southwest China. J Asian Earth Sci 38:65–75

Hendzel LL, Matthews CJD, Venkiteswaran JJ, Louis VLS, Burton D, Joyce EM, Bodaly RA (2005) Nitrous oxide fluxes in three experimental boreal forest reservoirs. Environ Sci Technol 39:4353–4360

Hinshaw SE, Dahlgren RA (2013) Dissolved nitrous oxide concentrations and fluxes from the eutrophic San Joaquin River, California. Environ Sci Technol 47:1313–1322

Hu Y, Cheng H (2013) The urgency of assessing the greenhouse gas budgets of hydroelectric reservoirs in China. Nature Clim Change 3:708–712

Huttunen JT, Vaisanen TS, Hellsten SK, Heikkinen M, Nykanen H, Jungner H, Niskanen A, Virtanen MO, Lindqvist OV, Nenonen OS, Martikainen PJ (2002) Fluxes of CH_4, CO_2, and N_2O in hydroelectric reservoirs Lokka and Porttipahta in the northern boreal zone in Finland. Glob Biogeochem Cycles. doi:10.1029/2000GB001316

Huttunen JT, Juutinen S, Alm J, Larmola T, Hammar T, Silvola J, Martikainen PJ (2003) Nitrous oxide flux to the atmosphere from the littoral zone of a boreal lake. J Geophys Res Atmos 108:4421. doi:10.1029/2002JD002989

IPCC (2006) IPCC guidelines for national greenhouse gas inventories. Prepared by the National Greenhouse Gas Inventory Program. Institute for Global Environmental Strategies, Hayama

Lerman A (1979) Geochemical processes. Water and sediment environments. John Wiley and Sons, Inc., Hoboken

Li SL, Liu CQ, Li J, Liu XL, Chetelat B, Wang BL, Wang FS (2010) Assessment of the sources of nitrate in the Changjiang River, China using a nitrogen and oxygen isotopic approach. Environ Sci Technol 44:1573–1578

Lima Id, Victoria R, Novo E, Feigl B, Ballester M, Ometto J (2002) Methane, carbon dioxide and nitrous oxide emissions from two Amazonian reservoirs during high water table. Internationale Vereinigung fur Theoretische und Angewandte Limnologie Verhandlungen 28:438–442

Liu CQ (2007) Biogeochemical processes and cycling of nutrients in the earth's surface: chemical erosion and nutrient cycling in Karstic catchments, Southwest China. Science Press, Beijing, p 608 **(in Chinese)**

Liu XL, Liu CQ, Li SL, Wang FS, Wang BL, Wang ZL (2011a) Spatiotemporal variations of nitrous oxide (N_2O) emissions from two reservoirs in SW China. Atmos Environ 45:5458–5468

Liu Y, Zhu R, Ma D, Xu H, Luo Y, Huang T, Sun L (2011b) Temporal and spatial variations of nitrous oxide fluxes from the littoral zones of three alga-rich lakes in coastal Antarctica. Atmos Environ 45:1464–1475

Liu XL, Bai L, Wang ZL, Li J, Yue FJ, Li SL (2015) Nitrous oxide emissions from river network with variable nitrogen loading in Tianjin, China. J Geochem Explor 157:153–161

McCrackin ML, Elser JJ (2011) Greenhouse gas dynamics in lakes receiving atmospheric nitrogen deposition. Glob Biogeochem Cycles 25:GB4005. doi:10.1029/2010GB003897

Mengis M, Gachter R, Wehrli B (1996) Nitrous oxide emissions to the atmosphere from an artificially oxygenated lake. Limnol Oceanogr 41:548–553

Mengis M, Gachter R, Wehrli B (1997) Sources and sinks of nitrous oxide (N_2O) in deep lakes. Biogeochemistry 38:281–301

Musenze RS, Fan L, Grinham A, Werner U, Gale D, Udy J, Yuan ZG (2016) Methane dynamics in subtropical freshwater reservoirs

and the mediating microbial communities. Biogeochemistry 128:233–255

Nevison C, Butler JH, Elkins JW (2003) Global distribution of N_2O and the Delta N_2O-AOU yield in the subsurface ocean. Glob Biogeochem Cycles 17:1119. doi:10.1029/2003GB002068

Peng X, Wang B, Liu C, Liu X, Wang F (2012) Diurnal variations of pCO_2 in relation to environmental factors in the cascade reservoirs along the Wujiang River, China. Chin J Geochem 31:41–47

Ravishankara AR, Daniel JS, Portmann RW (2009) Nitrous Oxide (N_2O): the dominant ozone-depleting substance emitted in the 21st century. Science 326:123–125

Rosenberg DM, McCully P, Pringle CM (2000) Global-scale environmental effects of hydrological alterations: introduction. Bioscience 50:746–751

Sasaki Y, Koba K, Yamamoto M, Makabe A, Ueno Y, Nakagawa M, Toyoda S, Yoshida N, Yoh M (2011) Biogeochemistry of nitrous oxide in Lake Kizaki, Japan, elucidated by nitrous oxide isotopomer analysis. J Geophys Res Biogeosci 116

Satterfield CN (1970) Mass transfer in heterogeneous catalysis. MIT Press, Cambridge

Seitzinger SP, Kroeze C (1998) Global distribution of nitrous oxide production and N inputs in freshwater and coastal marine ecosystems. Global Biogeochem Cycles 12:93–113

Sikar E, Santos M, Matvienko B, Silva M, Rocha C, Santos E, Bentes A, Rosa L (2005) Greenhouse gases and initial findings on the carbon circulation in two reservoirs and their watersheds. Proc Int Assoc Theor Appl Limnol 29:573

Sturm K, Yuan Z, Gibbes B, Werner U, Grinham A (2014) Methane and nitrous oxide sources and emissions in a subtropical freshwater reservoir, South East Queensland, Australia. Biogeosciences 11:5245–5258

Suntharalingam P, Sarmiento JL (2000) Factors governing the oceanic nitrous oxide distribution: simulations with an ocean general circulation model. Global Biogeochem Cycles 14:429–454

Wang SL, Liu CQ, Yeager KM, Wan GJ, Li J, Tao FX, Lue YC, Liu F, Fan CX (2009) The spatial distribution and emission of nitrous oxide (N_2O) in a large eutrophic lake in eastern China: anthropogenic effects. Sci Total Environ 407:3330–3337

Wang F, Wang B, Liu C-Q, Wang Y, Guan J, Liu X, Yu Y (2011) Carbon dioxide emission from surface water in cascade reservoirs-river system on the Maotiao River, southwest of China. Atmos Environ 45:3827–3834

Wang SL, Yeager K, Wan GJ, Liu CQ, Liu F, Lu YC (2015) Dynamics of CO_2 in a karst catchment in the southwestern plateau, China. Environ Earth Sci 73:2415–2427

Yu ZJ, Deng HG, Wang DQ, Ye MW, Tan YJ, Li YJ, Chen ZL, Xu SY (2013) Nitrous oxide emissions in the Shanghai river network: implications for the effects of urban sewage and IPCC methodology. Glob Change Biol 19:2999–3010

Zhu D, Chen H, Yuan X, Wu N, Gao Y, Wu Y, Zhang Y, Peng C, Qa Zhu, Yang G, Wu J (2013) Nitrous oxide emissions from the surface of the Three Gorges Reservoir. Ecol Eng 60:150–154